

Compact $\text{GdBa}_2\text{Cu}_3\text{O}_{7-\delta}$ coated conductor cables for electric power transmission and magnet applications

This article has been downloaded from IOPscience. Please scroll down to see the full text article.

2011 Supercond. Sci. Technol. 24 042001

(<http://iopscience.iop.org/0953-2048/24/4/042001>)

View [the table of contents for this issue](#), or go to the [journal homepage](#) for more

Download details:

IP Address: 132.163.52.47

The article was downloaded on 10/02/2011 at 19:33

Please note that [terms and conditions apply](#).

RAPID COMMUNICATION

Compact $\text{GdBa}_2\text{Cu}_3\text{O}_{7-\delta}$ coated conductor cables for electric power transmission and magnet applications*

D C van der Laan^{1,2}, X F Lu^{1,2} and L F Goodrich²¹ Department of Physics, University of Colorado, Boulder, CO 80309, USA² National Institute of Standards and Technology, Boulder, CO 80305, USAE-mail: danko@boulder.nist.gov

Received 23 November 2010, in final form 20 January 2011

Published 10 February 2011

Online at stacks.iop.org/SUST/24/042001**Abstract**

Bundling high-temperature superconductors together to form high-current cables is required in, for instance, power transmission and low-inductance magnet applications. Cabling techniques that have been applied so far have not resulted in compact, mechanically robust, high-current cables that remain flexible. Here, we demonstrate that the cabling technique that we have introduced only recently enables the construction of cables from high-temperature superconducting coated conductors that meet these requirements. We present details of a cable, wound from $\text{GdBa}_2\text{Cu}_3\text{O}_{7-\delta}$ coated conductors, that has an outer diameter of 7.5 mm and a critical current of about 2800 A at 76 K and self-field. The compact size and flexibility make the cable suitable for Navy and Air Force power transmission, and would allow superconducting power transmission lines that have been installed in the electric power grid to be reduced in diameter. The potential of increasing the engineering current density of the cable, while maintaining flexibility, makes them also suitable for high-field magnet applications.

(Some figures in this article are in colour only in the electronic version)

1. Introduction

High-temperature superconductors (HTS) are a practical alternative for replacing normal conducting materials in power grid applications, since their high critical temperature (T_c) allows them to be cooled with liquid nitrogen or helium gas. Because of their high upper critical field, HTS are also the only option for ultra-high-field magnets that operate above 25 T. Most of these applications require that the conductor be bundled to increase the overall current of either the transmission line or magnet winding.

Currently, HTS power grid transmission lines operate at a nominal current of up to 3 kA/phase and consist of a large number of superconducting tapes that are wound around a relatively large former. For instance, a three-phase cable

installed in Columbus, OH, features $\text{Bi}_2\text{Sr}_2\text{Ca}_2\text{Cu}_3\text{O}_x$ (Bi-2223) tapes that are wound around a large former, which results in a 7 cm diameter cable, carrying 3 kA RMS at around 73 K [1]. Another cable, installed in Albany, NY [2], featured a section where $\text{YBa}_2\text{Cu}_3\text{O}_{7-\delta}$ (YBCO)-coated conductors in each of the three phases are wound around a 1.6 cm former, resulting in a 3.5 cm diameter cable (per phase), which includes the dielectric, carrying 800 A rms at around 69 K. The relatively large diameter of these cables limits their flexibility and the total length of the cable that can be shipped by truck from the factory to the site of installation. HTS transmission lines that are currently installed in the electric power grid are not suitable for Navy and Air Force applications, because these applications require them to be very compact and lightweight [3, 4]. The same can be said for HTS cables that will potentially be used as magnet feeders in the Large Hadron Collider [5] or other facilities where many

* Contribution of NIST, not subject to US copyright.

superconducting magnets are connected in series. Operation under ac-current conditions also requires the cables to have low ac losses, which can be accomplished by, for instance, limiting the gaps between the individual conductors.

High-field magnets that are operated under relatively high-current ramp rates, such as in particle accelerators and fusion devices, require a low inductance and thus high-current windings. The ac losses of the cables should be limited to reduce the heat load on the cryogenic system during ramping, which in magnets can be accomplished by reducing the twist pitch of the conductors in the cable. In general, HTS cables for high-field magnets should meet the following criteria: they should have a high in-field engineering current density (J_e); be round, flexible and mechanically robust; have isotropic in-field properties and low ac losses; and preferably be constructed with conventional cabling techniques.

Currently, REBCO (rare earth barium cuprate)-coated conductors are produced in long lengths with high critical current densities (J_c) at 77 K, as well as at high magnetic fields at 4.2 K [6]. These conductors have proven to be mechanically strong; the conductor can withstand large axial tensile and compressive strains without mechanically degrading [7, 8]. Other HTS that may be used in high-field magnet applications include Bi-2223 tapes and $\text{Bi}_2\text{Sr}_2\text{CaCu}_2\text{O}_x$ (Bi-2212) wires. Bi-2212 wires have been previously bundled into Rutherford cables [9] for magnet applications, but the mechanical strength of Bi-2212 wires and Bi-2223 tapes is far below that of REBCO-coated conductors [10–13]. REBCO-coated conductors are therefore a prime candidate for HTS cables for power transmission and high-field magnet applications.

Initial approaches to cable REBCO-coated conductors include the Roebel-assembled coated conductor approach [14, 15], where multiple coated conductors are cut into strands that are then assembled into a rectangular cable. Although high cable current densities can be obtained this way, this approach is relatively costly, because a large fraction of the conductor is lost. Another cabling approach is through stacking multiple coated conductors in a rectangular structure [16]. Both approaches do not meet all the above-mentioned criteria for magnet cables; the cables are rectangular, not very flexible and have anisotropic in-field properties.

We have recently introduced an approach to cable YBCO-coated conductors by spiral-winding them on a small, round former with the YBCO layer on the inside (under axial compression) [17]. This method results in a compact cable that likely meets all of the requirements for compact power transmission cables and high-field magnet windings. Here we further demonstrate the feasibility of the compact cable concept by constructing several single- and multi-layer cables with GBCO-coated conductors. The performance of the cables is tested as a function of cable bend radius, demonstrating its high degree of flexibility. We constructed a high-current, single-phase cable to demonstrate the possibility of lightweight HTS power transmission.

2. Experiment

GBCO-coated conductors manufactured by SuperPower Inc. consisted of ceramic buffer layers deposited on a 50 μm thick

Hastelloy C-276 substrate. During fabrication, grain alignment is introduced into the MgO buffer layer with ion-beam-assisted deposition (IBAD), and a 1.0 μm thick $\text{GdBa}_2\text{Cu}_3\text{O}_{7-\delta}$ layer is deposited on top of the buffer layers by metal-organic chemical vapor deposition (MOCVD) [18, 19]. A silver cap layer, 2–3 μm thick, is deposited on top of the GBCO layer for electrical stability. The coated conductors are slit from a 12 mm wide tape to their final width of 4 mm. They are surround-plated with 20 μm of copper for electrical and thermal stability. Samples from two different batches were used. The critical current density at 76 K and self-field of the GBCO conductor from batch 1 was about 2.5 MA cm^{-2} and that from batch 2 was about 3.0 MA cm^{-2} .

The dependence of the critical current (I_c) of the coated conductors on axial strain was measured at 76 K. The samples were soldered onto the surface of 98wt%Cu–2wt%Be (CuBe) beams by use of 97wt%In–3wt%Ag solder with a melting temperature of 143 °C. Axial strain was applied by bending the beams in a four-point bender [7]. The critical current was determined by a four-contact measurement with an uncertainty of about $\pm 0.5\%$ at an electric field criterion of 1 $\mu\text{V cm}^{-1}$. Strain was measured directly with strain gauges mounted on top of the beams and on top of the samples.

Coated conductor cables were constructed by spiral-winding multiple conductors around an insulated, flexible, round, copper cable that had an outer diameter of 5.5 mm and was surrounded by a layer of nylon insulation. Each superconducting layer was wound by hand in the direction opposite to the winding direction of its neighboring layer. The coated conductors of the cable were soldered with 97wt%In–3wt%Ag solder to brass or copper lugs that act as current contacts. One set of voltage contacts was soldered in the middle of one of the coated conductors located in the outer layer of each cable. A second set of voltage contacts was soldered on the current contacts and was connected to a quench detector. Some of the cables were bent over a fixed bending radius at room temperature and attached to a fiberglass board before the critical current was measured at 76 K.

3. Results

3.1. Effect of strain on I_c of GBCO-coated conductors

The inward facing superconducting layer of a GBCO-coated conductor will be placed under axial compression when spiral-wound on a round former [17]. Since I_c changes reversibly with strain [7], we expect that the performance of the conductor in the cable is different from that of a straight sample. Also, there is a possibility that the conductor becomes mechanically damaged when the compressive strain exceeds a certain level. Hence, we must measure the strain dependence of I_c of each batch of conductors used to construct a cable.

The strain dependence of I_c as a function of tensile and compressive strain that was measured on two straight GBCO samples from batch 2, which were soldered on a bending beam, is shown in figure 1. The critical current shows a broad maximum around 0% strain. The irreversible strain limit under tension ($\epsilon_{\text{irr,ten}}$) at which I_c degrades irreversibly is reached

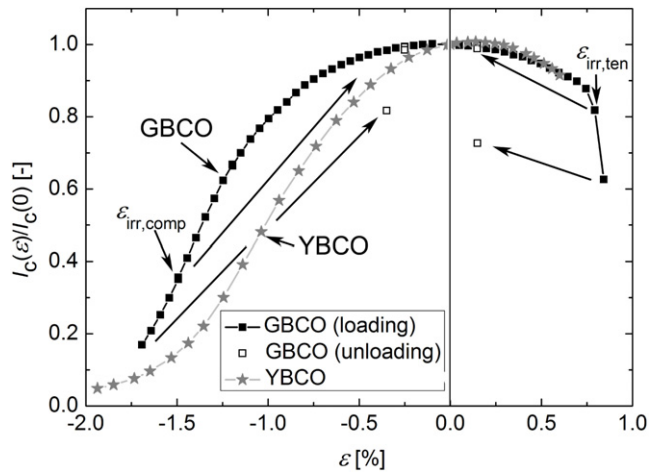


Figure 1. Strain dependence of I_c , normalized to its value at 0% applied strain, of two GBCO samples from batch 2. The strain dependence of I_c of two YBCO samples from [17] is included in the figure for comparison. In both cases, one sample was measured under compression and a second sample was measured under tension. In the case of the GBCO samples, $\varepsilon_{irr,ten}$ and $\varepsilon_{irr,comp}$ are indicated in the figure and arrows indicate from which point the strain was unloaded to verify reversibility. In the case of the YBCO samples, only reversible data are shown.

at 0.75% strain. Mechanical damage occurs when the strain exceeds this value, which becomes clear when I_c does not recover after the strain is unloaded (open squares). The strain dependence of I_c of a second sample from the same batch was measured as a function of compressive strain. I_c is reduced gradually under compressive strain (solid squares) and fully recovers when the strain is unloaded (open squares), up to a strain of between -1.5% and -1.7% . The irreversible strain limit under compression ($\varepsilon_{irr,comp}$) is thus -1.5% , since the last full recovery of I_c was measured when unloading from this strain value.

The dependence of I_c on compressive strain of two YBCO samples from the conductor batch that was used in our previous cabling work [17] is included in figure 1 for comparison. The strain dependences of YBCO- and GBCO-coated conductors have important differences. First, the YBCO-coated conductors in [17] showed no irreversible degradation under compressive strain up to a strain of -2% . Second, the peak in I_c in the GBCO samples is reached at 0% strain, whereas the peak in I_c of the YBCO samples is reached at 0.15% tension. Third, I_c of the YBCO-coated conductors in [17] is more sensitive to strain than I_c of the GBCO-coated conductors. For example, I_c of the YBCO-coated conductors is reduced by about 50% at -1% compressive strain, whereas I_c of the GBCO-coated conductors is reduced by only 23% at that strain level. These differences have consequences for the performance of cables that are constructed from these conductors. In the case of the GBCO-coated conductor, it is important that the total compressive strain applied to the conductor when wound around the former, plus additional compressive strain that may be introduced during bending and cool-down of the cable, does not exceed -1.5% . The performance of GBCO-coated conductors when wound into a

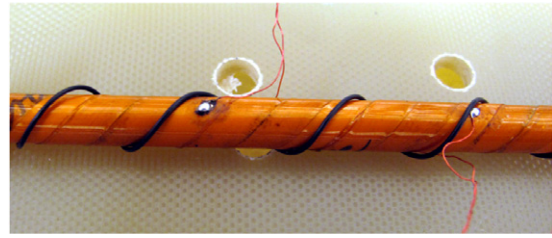


Figure 2. A single-layer cable prepared by winding three conductors (one GBCO-coated conductor and two dummy conductors) in parallel around a 5.5 mm former. One set of voltage contacts was connected to the middle of the cable and a second set was connected to the copper current terminals. One of the voltage wires from the second set was wound around the cable with the same twist pitch as the coated conductors to reduce voltage noise.

Table 1. Compact GBCO cables.

Cable #	Number of layers	Number of conductors	Batch number	I_c (A) (76 K)
1	1	1	1	98.5
2	4	12	1	1232
3	8	24	2	2796

cable is expected to be superior to that of the YBCO-coated conductors because I_c of the GBCO-coated conductors is much less affected by strain.

3.2. Effect of bending on the cable I_c

Besides the strain that is introduced by winding the coated conductors on a round former, large strains can be introduced into the GBCO layer during cable bending. During cable bending, tensile strain is applied to the outside while compressive strain is applied to the inside of the bend. This added strain could potentially damage the GBCO-coated conductor if the total strain exceeds the irreversible strain limit under either compression or tension.

A one-layer cable (cable 1 in table 1) was prepared to investigate the effect of cable bending on the performance of the GBCO conductors in the cable. The cable consists of one GBCO-coated conductor from batch 1, with a critical current of 99.5 A at 76 K, and two dummy conductors wound in parallel around a 5.5 mm former (see figure 2). The dummy conductors were 4 mm wide, 50 μm thick, Hastelloy C-276 tapes that were surround-plated with 20 μm of copper but that have no superconducting layer. The three conductors were wound with a twist pitch of about 34 mm. The strain applied to the GBCO layer along the direction of the current can be calculated from equations (2) in [17] and is -0.46% . This would lead to a reduction in I_c of only 3.6%, based on the measurement presented in figure 1. The critical current of the straight cable is 98.5 A at 76 K (see figure 3), which is very close to that of the straight coated conductor.

When the cable with 5.5 mm diameter former is bent around a radius r , the bending strain on the surface of the former, along the direction of the cable, is equal to $\varepsilon = \pm 0.055/2r$ (see equations (1a), and (1b) in [8]). A bending

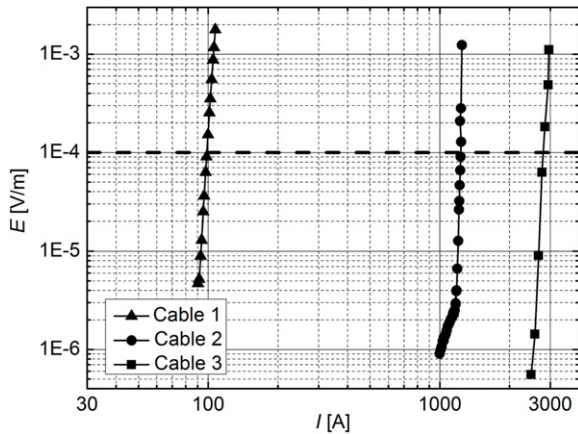


Figure 3. Electric field as a function of current of cables 1, 2 and 3. The electric-field criterion of $1 \mu\text{V cm}^{-1}$ is indicated by the dashed line. Only the E - I curves measured with the voltage contacts that were connected to the center of each cable are shown.

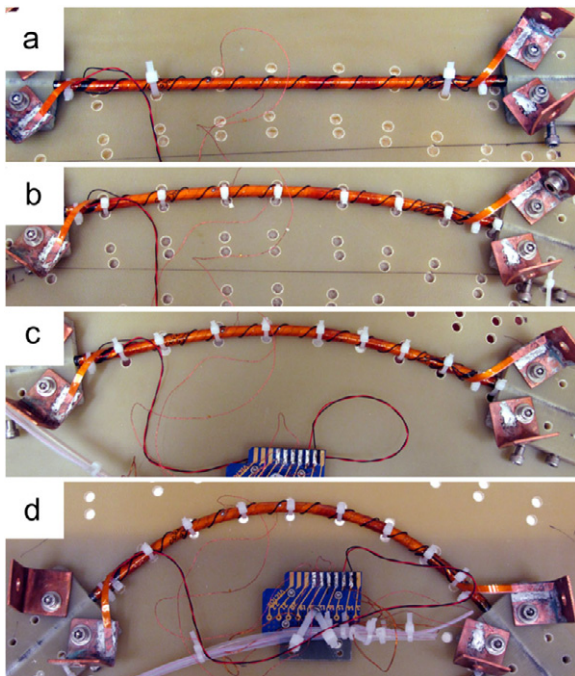


Figure 4. The single-layer cable (cable 1) is bent at room temperature around a radius r and fixed to a fiberglass plate before being cooled to 76 K. (a) Straight cable. (b) Bending radius $r = 0.5$ m, (c) $r = 0.25$ m and (d) $r = 0.125$ m.

radius of 27.5 cm would result in a bending strain at the surface of the former of $\pm 1\%$. The added bending strain would bring the total strain in the GBCO layer on the inside of the bend close to $\epsilon_{\text{irr,comp}}$ of -1.5% , if all bending strain were transferred from the former into the GBCO layer. To measure the effect of cable bending on I_c , cable 1 was bent over a radius of 0.5 m at room temperature (see figure 4) before it was cooled to 76 K. The cable was warmed to room temperature after I_c was measured, after which it was bent over a smaller radius. This procedure was repeated for decreasing bending radii.

Bending of the cable did not affect the critical current, even when the cable was bent over a radius of 12.5 cm (see

Table 2. Critical current of cable 1 as a function of bending radius.

Bending radius (m)	Bending strain ^a (%)	I_c (A)
∞	0	98.5
0.5	± 0.55	98.8
0.375	± 0.73	96.7
0.25	± 1.1	97.6
0.125	± 2.2	98.9

^a The \pm sign indicates both compressive ($-$) strain on the inside of the bend and tensile ($+$) strain on the outside of the bend.

table 2), which corresponds to a bending strain on the surface of the former of $\pm 2.2\%$. Even though the bending strain on the surface of the former is relatively large, it is not transferred to the coated conductor that is spiral-wound around it. The coated conductor is able to slide over the former from the compressive side of the cable to the tensile side, thereby greatly reducing the additional build-up of strain.

3.3. Compact high-current GBCO cables

Several multi-layer cables were constructed (see table 1) to demonstrate the potential of the cabling method for flexible, compact cables for power transmission. The first high-current cable (cable 2) consisted of four layers that each contained three conductors of batch 1 in parallel. The conductors were spiral-wound around a 5.5 mm former (figure 5), with each additional layer spiral-wound in the direction opposite to that of the previous layer. A layer of polyamide tape was applied on the outside of the fourth layer, bringing the cable outer diameter to 6.5 mm, which results in a packing factor of about 90%. Brass current contacts were attached to the former with nylon screws, preventing the copper core of the former to be in electrical contact with the current terminals.

The cable was bolted to a fiberglass plate and cooled to 76 K in liquid nitrogen after four thick copper cables were connected to each current contact (figure 6(a)). Each coated conductor used to wind the cable had an I_c of about 100 A. The cable critical current of 1232 A (see figure 3), with an n value of 75.8 (which is an indication of the steepness of the superconducting transition), was measured by use of the set of voltage taps connected to the center of the cable.

The cable was bent over a radius of 12.5 cm at room temperature to demonstrate its flexibility. After the cable was bolted to the fiber glass plate (figure 6(b)) and cooled, the I_c was measured again. The cable I_c at a bending radius of 12.5 cm was 1239.8 A with an n value of 60.2.

A second high-current cable was constructed (cable 3) by spiral-winding 24 conductors from batch 2 in eight layers (three conductors per layer) around a former with 5.5 mm outer diameter. The outer diameter of the cable, with one layer of polyamide tape on its outside, was 7.5 mm (a packing factor of about 90%). Large, tapered, cylindrical copper current lugs were attached (figure 7) to accommodate the higher expected cable critical current. The individual coated conductors have an I_c of about 125 A at 76 K. The cable critical current was 2796 A (see figure 3), which is on average 116.5 A per conductor. The

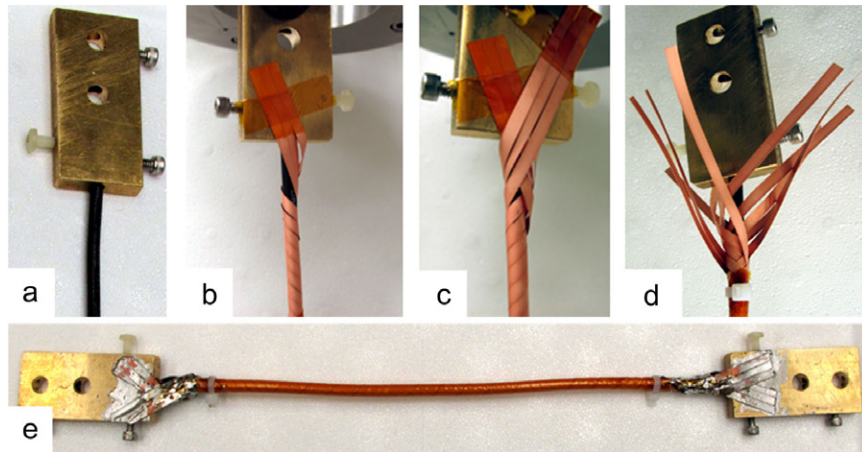


Figure 5. Construction of a four-layer high-current cable (cable 2). (a) Brass current contacts were bolted to the 5.5 mm diameter former. (b) The first layer of three conductors is wound. (c) The second layer is wound. (d) All four layers are wound. (e) The coated conductors are soldered to each side of the brass current terminals.

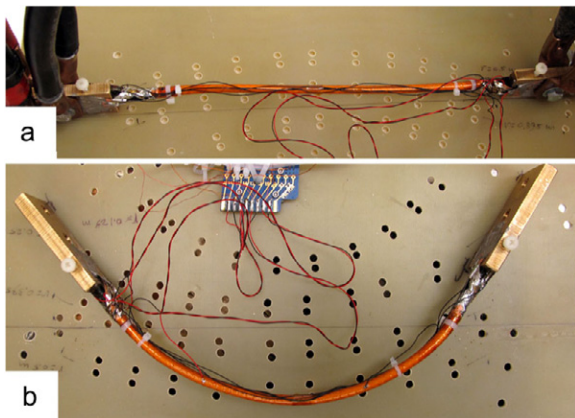


Figure 6. (a) Cable 2 being installed for testing. (b) Cable 2 bent over a 12.5 cm radius.

cable current was increased above I_c to the maximum current of the power supply of 2960 A without inducing a quench.

A replica of cable 3 was constructed with 24 dummy conductors, which were Hastelloy C-276 tapes surrounded with copper, with the same dimensions as the coated conductors used in cable 3, but without the superconducting layer. The replica cable was cast in epoxy, cut and polished. An optical micrograph of its cross section is shown in figure 8. The copper strands within the former are clearly visible, together with the 24 conductors of the eight layers. Although the cable was wound by hand, there is an average spacing of only 20–30 μm between the layers, which can be clearly seen in the magnification of part of the coated conductor stack in figures 8(b) and (c).

4. Discussion

The importance of studying the reversible effect of strain on I_c in coated conductors, and its impact on applications, becomes clear when the strain dependence of I_c of YBCO-coated conductors is compared with that of GBCO-coated conductors. The I_c of GBCO-coated conductors is reduced by

only a few per cent when wound into a compact cable with a 5.5 mm diameter former, thereby experiencing -0.5% strain, compared with an expected degradation of 15% in the case of YBCO-coated conductors. The relatively low strain sensitivity of I_c therefore makes GBCO-coated conductors superior for use in compact coated conductor cables.

The prototype compact cables that were constructed with GBCO-coated conductors demonstrated the potential to make practical high-current cables that remain flexible. Cable flexibility is important when transmission lines are pulled through conduits that have tight bends, which is likely to occur in Navy and Air Force applications. Flexibility is even more important for winding magnets, since the inner diameter of high-field magnets may be relatively small. We demonstrated that a relatively thick cable with an outer diameter of 6.5 mm showed no degradation in I_c when bent over a radius as small as 12.5 cm. Since the conductors are not glued or soldered onto the former and are able to adjust their position, no noticeable stress builds up on the coated conductors in the cable when the cable is bent. This suggests that a bending radius smaller than 12.5 cm could be applied to the cable before significant degradation occurs.

The coaxial configuration of the cable has important implications for its performance. This configuration shields the cable interior from its self-field, largely reducing the magnetic field component perpendicular to the surface of the coated conductors in the cable. This shielding explains the relatively high n value of the cable (75.8 for cable 2), compared with that of a single coated conductor, which is around 35. Slight gaps between the conductors may develop upon cable bending, reducing the level of shielding, which explains the reduction in n value from 75.8 to 60.2 when the cable was bent over a radius of 12.5 cm. The self-shielding of the cable could potentially reduce the transport ac losses of the cable. The effect of the cable configuration on ac losses will be investigated in future studies.

Cable 3 has a critical current of almost 2800 A at 76 K, and is expected to have a critical current of about 4800 A at 65 K (pumped nitrogen) with a single-phase cable diameter

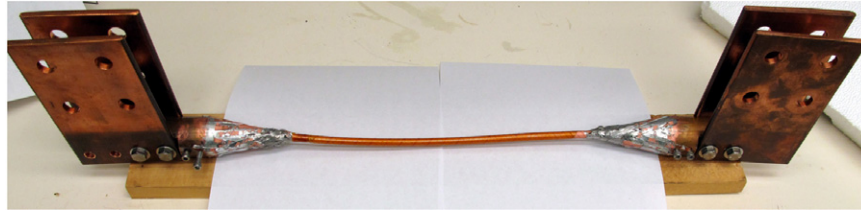


Figure 7. High-current cable 3 with installed copper current contacts.

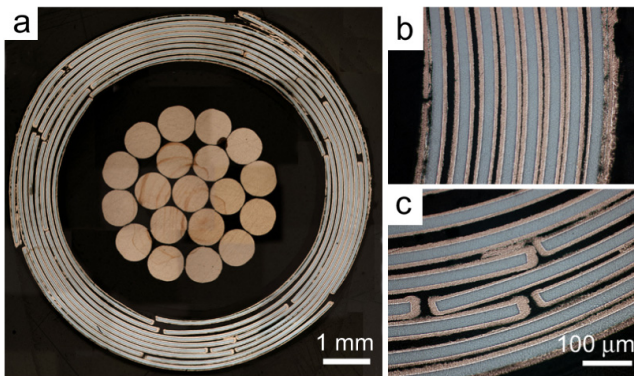


Figure 8. (a) Optical micrograph (5 \times magnification) of the cross section of a replica of cable 3. The cable consists of eight layers with three dummy conductors each that are wound around a 5.5 mm former. The copper strands of the former are visible in the center of the cable. (b) A high magnification image (10 \times) of part of the conductor stack shows small gaps between the individual layers and (c) between the conductors in each layer.

of only 7.5 mm. This is the same, or higher, current capacity than reached by much larger demonstration HTS power transmission cables that are currently installed in the electric power grid. A significant reduction in size and weight can thus be achieved by use of the compact cable design.

5. Conclusions

The potential of the recently introduced compact coated conductor cable concept has further been demonstrated by constructing high-current cables with $\text{GdBa}_2\text{Cu}_3\text{O}_{7-\delta}$ coated conductors. The performance of $\text{GdBa}_2\text{Cu}_3\text{O}_{7-\delta}$ coated conductors is superior to that of $\text{YBa}_2\text{Cu}_3\text{O}_{7-\delta}$ coated conductors in cables, because the critical current density of $\text{GdBa}_2\text{Cu}_3\text{O}_{7-\delta}$ is less sensitive to strain. The cable flexibility was demonstrated by bending a 6.5 mm diameter cable over a radius as small as 12.5 cm, which did not reduce the critical current. A high-current cable with a critical current of 2796 A at 76 K was constructed. The cable carried a similar, or larger, amount of current compared to that of high-temperature superconducting transmission lines currently installed in the electric power grid, but with a much smaller cable diameter of only 7.5 mm.

Acknowledgments

The authors thank Ted Stauffer and Fraser Douglas for their technical support, and SuperPower Inc. for providing the

copper-plated Hastelloy C-276 substrate used as the dummy conductor. This work was supported in part by the US Department of Energy, Office of Electricity Delivery and Energy Reliability. Certain commercial materials are referred to in this paper to foster understanding. Such identification implies neither recommendation nor endorsement by NIST, nor that the materials identified are necessarily the best available for the purpose.

References

- [1] Demko J A *et al* 2007 *IEEE Trans. Appl. Supercond.* **17** 2047
- [2] Yumura H, Ashibe Y, Itoh H, Ohya M, Watanabe M, Masuda T and Weber C S 2009 *IEEE Trans. Appl. Supercond.* **19** 1698
- [3] Haugan T J, Long J D, Hampton L A and Barnes P N 2008 *SAE Int. J. Aerosp.* **1** 1088–94
- [4] Fitzpatrick B K, Golda E M and Kephart J T 2008 *Adv. Cryog. Eng.* **53** 277–83
- [5] Ballarino A, Meß K H and Taylor T 2008 *IEEE Trans. Appl. Supercond.* **18** 1455
- [6] Selvamanickam V, Chen Y, Xie J, Zhang Y, Guevara A, Kesgin I, Majkic G and Martchevsky M 2009 *Physica C* **469** 2037
- [7] van der Laan D C and Ekin J W 2007 *Appl. Phys. Lett.* **90** 052506
- [8] van der Laan D C and Ekin J W 2008 *Supercond. Sci. Technol.* **21** 115002
- [9] Scanlan R M, Dietderich D R, Higley H C, Marken K R, Motowidlo L R, Sokolowski R and Hasegawa T 1999 *IEEE Trans. Appl. Supercond.* **9** 130
- [10] Ekin J W, Finnemore D K, Li Q, Tenbrink J and Carter W 1992 *Appl. Phys. Lett.* **61** 858–60
- [11] tenHaken B, Godeke A, Schuver H J and tenKate H H J 1996 *IEEE Trans. Magn.* **32** 2720
- [12] van der Laan D C, van Eck H J N, ten Haken B, ten Kate H H J and Schwartz J 2003 *IEEE Trans. Appl. Supercond.* **13** 3534
- [13] van der Laan D C, Ekin J W, van Eck H J N, Dhalte M, ten Haken B, Davidson M W and Schwartz J 2006 *Appl. Phys. Lett.* **88** 022511
- [14] Goldacker W, Nast R, Kotzyba G, Schlachter S I, Frank A, Ringsdorf B, Schmidt C and Komarek P 2006 *J. Phys.: Conf. Ser.* **43** 901–4
- [15] Goldacker W, Frank A, Kudymow A, Heller R, Kling A, Terzieva S and Schmidt C 2009 *Supercond. Sci. Technol.* **22** 034003
- [16] Ando T and Nishio S 2005 *21st IEEE/NPSS Symp. on Fusion Engineering* pp 151–4
- [17] van der Laan D C 2009 *Supercond. Sci. Technol.* **22** 065013
- [18] Selvamanickam V *et al* 2001 *IEEE Trans. Appl. Supercond.* **11** 3379
- [19] Selvamanickam V, Xie Y, Reeves J and Chen Y 2004 *MRS Bull.* **29** 579